Molecular Dynamics Hot Paper

International Edition: DOI: 10.1002/anie.201505890
German Edition: DOI: 10.1002/ange.201505890

Velocity of a Molecule Evaporated from a Water Nanodroplet: Maxwell–Boltzmann Statistics versus Non-Ergodic Events

Hassan Abdoul-Carime, Francis Berthias, Linda Feketeová, Mathieu Marciante, Florent Calvo, Valérian Forquet, Henry Chermette, Bernadette Farizon, Michel Farizon, and Tilmann D. Märk*

Abstract: *The velocity of a molecule evaporated from a mass-selected protonated water nanodroplet is measured by velocity map imaging in combination with a recently developed mass spectrometry technique. The measured velocity distributions allow probing statistical energy redistribution in ultimately small water nanodroplets after ultrafast electronic excitation. As the droplet size increases, the velocity distribution rapidly approaches the behavior expected for macroscopic droplets. However, a distinct high-velocity contribution provides evidence of molecular evaporation before complete energy redistribution, corresponding to non-ergodic events.*

The evaporation of water occurs through the breaking of one or several hydrogen bonds. These hydrogen bonds are responsible for many of the remarkable features of water[1] that are essential to life. Water is known for its exceptional ability to absorb and hold heat at the macroscopic level, whereas at the sub-microscopic level, the intermolecular transfer of vibrational energy is known to be ultrafast because of the strong interactions between O–H oscillators.[2,3] The quantitative description of energy transfer in hydrogen-bonded compounds after electronic excitation is particularly challenging. For a large water droplet, the evaporation of water manifests itself as a velocity distribution of the evaporated molecules obeying Maxwell–Boltzmann (MB) statistics as a result of energy equipartitioning in a thermalized system. In the present letter we address the thermalizing ability of even a small water droplet following the sudden excitation of one of its molecules.

Protonated water nanodroplets, $H^+(H_2O)_{n=2-8}$, are produced by supersonic expansion followed by electron impact ionization and acceleration at 8 keV energy. They are then mass- and velocity-selected more than 1 μs after being formed.[4] A single high-velocity collision (with $\mathbf{V_i}$ in the laboratory frame ranging from 10^5 to 2.10^5 ms^{-1}) with an Ar atom leads to energy deposition in the droplet by electronic excitation[5] of one of the molecules on a typical time scale of a fraction of a femtosecond.[6] High-velocity collisions[7,8] probe a broad range of energy deposition, in contrast to

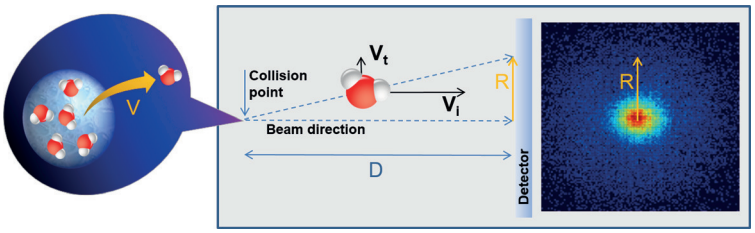

Figure 1. Velocity map imaging of molecules evaporated from water nanodroplets. Evaporation is induced by a single collision between a mass-selected protonated water nanodroplet and an argon atom. The nanodroplet has a selected laboratory-frame velocity $\mathbf{V_i}$ before the collision. The evaporated H_2O molecule acquires an additional transverse velocity, $\mathbf{V_t}$, (with respect to the original flight direction of the droplet) and reaches the detector placed at a distance $D = 250$ mm from the collision point. The impact position, R, of the evaporated molecule on the detector is related to the velocity, $\mathbf{V}$, of the evaporated molecule in the center-of-mass reference frame of the nanodroplet.

[*] Assist. Prof. Dr. H. Abdoul-Carime, F. Berthias, Dr. L. Feketeová, Dr. M. Marciante, Dr. V. Forquet, Prof. Dr. H. Chermette, Dr. B. Farizon, Prof. Dr. M. Farizon
Université de Lyon, 69003 Lyon (France)
E-mail: m.farizon@ipnl.in2p3.fr

Assist. Prof. Dr. H. Abdoul-Carime, F. Berthias, Dr. L. Feketeová, Dr. M. Marciante, Dr. V. Forquet, Prof. Dr. H. Chermette, Dr. B. Farizon, Prof. Dr. M. Farizon
Université Claude Bernard Lyon1
69622 Villeurbanne (France)

Assist. Prof. Dr. H. Abdoul-Carime, F. Berthias, Dr. L. Feketeová, Dr. B. Farizon, Prof. Dr. M. Farizon
Institut de Physique Nucléaire de Lyon
CNRS/IN2P3 UMR 5822, 43 Bd du 11 novembre 1918
69622 Villeurbanne Cedex (France)

Dr. M. Marciante
Institute Lumière Matière, CNRS
69622 Villeurbanne (France)

Dr. F. Calvo
Université Grenoble 1, CNRS, LIPhy UMR 5588
38041 Grenoble (France)

Dr. V. Forquet, Prof. Dr. H. Chermette
Institut des Sciences Analytiques, CNRS UMR 5280
43 boulevard 11 novembre
69622 Villeurbanne Cedex (France)

Prof. Dr. T. D. Märk
Institut für Ionenphysik und Angewandte Physik
Leopold Franzens Universität
6020 Innsbruck (Austria)

Supporting information for this article is available on the WWW under http://dx.doi.org/10.1002/anie.201505890.

laser experiments in which the selection of a specific excited state is possible.[2,3,9] The amount of deposited energy ranges from 0 to 12 eV (80% below 4 eV)[10] and therefore can be much higher than the binding energy of a molecule in the droplet (typically 1.37 eV for $n=2$, 0.85 eV for $n=3$, 0.78 eV for $n=4$, and 0.55 eV for $n>4$).[11] After excitation, the out-of-equilibrium nanodroplet relaxes through the evaporation of one or several molecules. The protonated fragment is mass analyzed at least 80 ns after the collision. The typical time required for evaporation is a few picoseconds,[12] and further evaporation after the mass analysis of the residue is negligible. The total kinetic energy released (KER) during the dissociation is partitioned because of momentum conservation, that is, the evaporated molecule acquires an additional velocity randomly oriented in the center-of-mass reference frame (CMF) of the parent droplet. Differently from previous mass spectrometric measurements of the average kinetic energy release in decaying metastable water cluster ions,[13] the present experiment combines velocity map imaging with the correlated ion and neutral time-of-flight mass spectrometry technique on an event-by-event basis[14–16] (COINTOF MS). Measurements are performed on a large number of individual droplets (typically 10^6) thereby obtaining the velocity distribution.

For the evaporated molecule, the additional velocity in the CMF leads to a transverse velocity component in the laboratory reference frame and consequently to a change in the impact position in the detection plane (Figure 1). The measured impact distribution, $P(R)$, is related to the velocity distribution, $f(V)$, of the water molecules in the CMF by Equation (1),

$$P(R) = \iint f(V)F(V,R_0)F_f(R_0 - R)\mathrm{d}V\mathrm{d}R_0 \qquad (1)$$

where $F(V, R_0)$ is the projection factor for an infinitely thin incident droplet beam centered at R_0 and $F_f(R_0-R)$ is the beam shape factor. Figure 2a–c shows the measured 2D impact distributions of the evaporated molecules after the selection of $H^+(H_2O)_4$ droplets evaporating one, two, and three molecules, respectively. The 2D impact distribution of the non-dissociated droplets obtained from the same dataset is presented in Figure 2d. These distributions of evaporated molecules exhibit radial symmetry, and the impact position of an evaporated molecule can be characterized in terms of the distance, R, between the impact point and the centroid of the distribution. Figure 2e shows the impact distributions, $P(R)$, plotted as a function of R, thus allowing for a quantitative comparison among the measured results for the evaporation of one, two, and three molecules. It is immediately clear that the impact distributions of the evaporated molecules are broader than that of the non-dissociated droplets. The width and most probable value of the measured impact distribution both increase with an increase in the number of molecules evaporated from $H^+(H_2O)_4$. The velocity distributions, $f(V)$, recovered from the recorded impact positions via Equation (1) are presented in Figure 2f and range from 0 to 10^4 ms^{-1}. In addition, the experimental velocity distributions for the evaporation of one molecule from protonated droplets containing $n=2$–8 molecules are presented in Figure 3. For all droplet sizes, the velocity distribution shows a well-defined

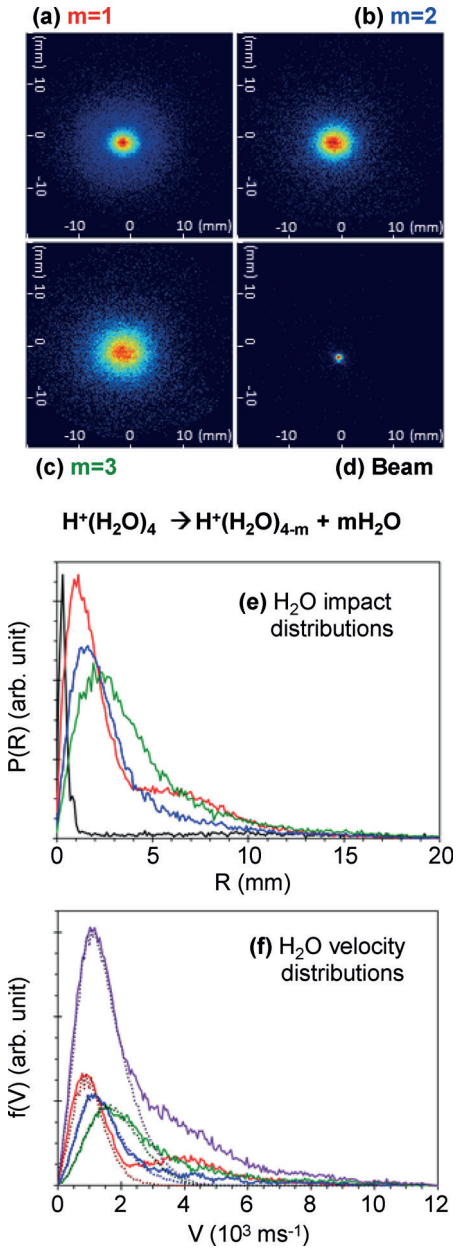

Figure 2. Impact and velocity distributions of molecules evaporated from $H^+(H_2O)_4$ droplets. a–c) Normalized 2D impact distributions of the evaporated molecules after the selection of $H^+(H_2O)_4$ droplets leading to the evaporation of exactly one (red: $m=1$), two (blue: $m=2$) or three (green: $m=3$) H_2O molecules. d) 2D impact distribution of the non-dissociated $H^+(H_2O)_4$ droplets (black: beam). In (a–d) all 2D impact distributions are normalized to their maximum values. e) Impact distributions, $P(R)$, plotted as a function of the distance R between the impact point and the centroid of the distribution. The areas under the curves are proportional to the branching ratios.[14] The black curve, which is normalized to the maximum value attained by the red curve, corresponds to the impact of the non-dissociated beam. f) H_2O velocity distributions recovered from the recorded impact positions (continuous lines, red: $m=1$, blue: $m=2$, green: $m=3$; the violet continuous line represents their sum). The corresponding dotted lines are the velocity distributions calculated via statistical molecular dynamics simulations.

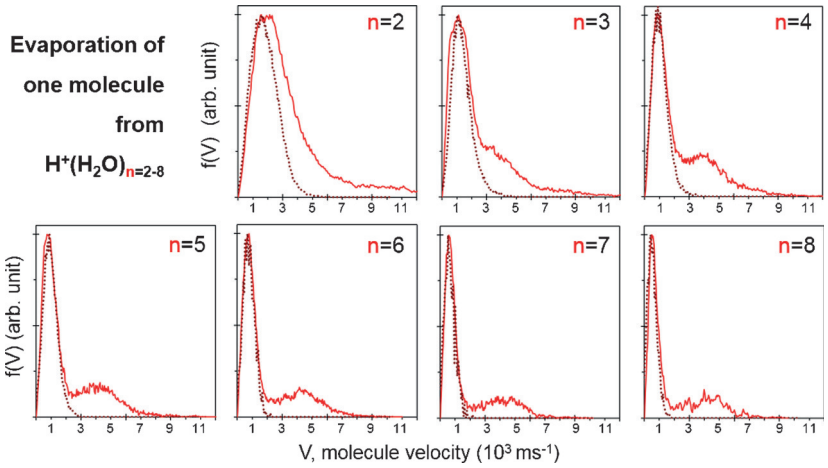

Figure 3. Normalized velocity distributions after the evaporation of one molecule from $H^+(H_2O)_{n=2-8}$ droplets. The experimental data are plotted as continuous lines, and the SMD simulation results are plotted as dotted lines. Typically, a molecule with a velocity of 2×10^3 ms^{-1} carries away a kinetic energy of 0.37 eV in the CMF.

sharp peak at smaller velocities that shifts towards lower velocities as the droplet size increases. When comparing with the dimer case (Figure 3, $n=2$), the summed velocity distribution observed for the tetramer (Figure 2(f)) is clearly shifted toward lower velocities. The molecules evaporated from larger clusters are translationally slower, thereby revealing the energy redistribution before evaporation. For $n=4$–8, the sharp low-velocity peak is well-fitted by a MB velocity distribution. Together, these findings highlight that energy redistribution prevails, demonstrating that despite clear differences in composition and acidity, evaporation in a small nanodroplet is similar to that in bulk water.

These observations are supported by statistical molecular dynamics (SMD) simulations performed using a flexible and polarizable potential[17,18] but neglecting intermolecular proton transfer. In these simulations, the nanodroplets are initially thermalized at 100 K. At the initial time, a random internal excitation energy drawn from a flat distribution in the 2–8 eV range is converted into atomic kinetic energy. In doing so, a complete conversion of the excitation energy into vibrations is assumed, as well as a complete statistical redistribution among all modes. All molecular dynamics trajectories employ a time step of 0.25 fs. After 1 ns, the various possible fragments are identified based on simple distance criteria, and their kinetic energies are calculated. An example of the sequential evaporation of two molecules from the tetramer is shown in the Supporting Information.[19] As in our experiment, the events are sorted according to the number of molecules evaporated at the time of detection. Repeating the analysis over 10^5 independent trajectories for each nanodroplet size yields velocity distributions that can be compared to the measurements under the assumption of the complete redistribution of the excitation energy. Additional simulations performed with the reactive OSS2 potential[20] produce no significant difference in the velocity distributions.[19] As seen in Figures 2 and 3, the theoretical calculations (shifted by a constant value of -740 ms^{-1} to account for the shorter detection window used in the simulation) well reproduce the behavior of the distribution function at low velocities. For a more quantitative comparison, Figure 4 illustrates the agreement and evolution of the distribution as a function of the droplet size n, where the calculated and measured values of the mean $\langle V\rangle$ and the full-width-at-half-maximum ΔV are both observed to decrease and saturate with an increasing number of molecules in the droplet. The present results for $\langle V\rangle$ are also in good agreement with the values obtained by Rybkin et al.[12] using large-scale Born–Oppenheimer molecular dynamics simulations (BOMD) for protonated water droplets near the magic number $n=21$. They are also consistent with the conclusions reached by Varilly and Chandler in the bulk limit.[22]

For the dimer and trimer, the experimental values of ΔV are significantly higher

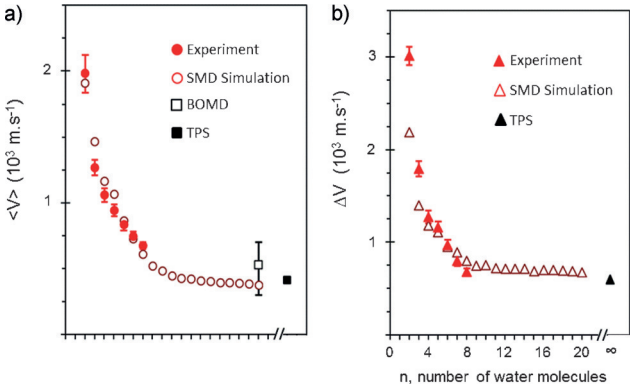

Figure 4. Mean values and full widths at half maximum of the H_2O velocity distributions. a) The mean values ($\langle V\rangle$) and b) the widths (ΔV) of the H_2O velocity distributions corresponding to the evaporation of one molecule from $H^+(H_2O)_{n=2-8}$. The full red symbols represent experimental data, and the empty red symbols represent the results of the present SMD simulations. The empty black symbol corresponds to the theoretical result obtained by Rybkin et al.[12] based on ab initio molecular dynamics trajectories (BOMD). The full black symbols correspond to the transition path sampling study (TPS) for a bulk sample of 900 water molecules by Varilly and Chandler.[22]

than those predicted by the statistical model. Moreover, it is interesting to note that the velocity distributions obtained in this case exhibit much larger $\langle V\rangle$ and ΔV values compared with those measured by Samanta et al.[21] for the neutral water dimer and trimer (in the trimer case: $\langle V\rangle\approx300$ ms^{-1}, $\Delta V\approx250$ ms^{-1}). In the cited study using infrared laser excitation, the deposited energies were much smaller than those involved in the high-energy collisions of the present study. Because of the COINTOF technique used here, single-molecule evaporation can be specifically selected from among all the collision-induced evaporation events. Since these events span the entire regime where none to all water molecules are evaporated, the measured velocity distributions of the present study (Figure 3) represent the most extensive data

that one can expect for the evaporation of one molecule after complete energy redistribution.

In addition to the dominant statistical contribution, the experimental distributions also reveal evaporated molecules with velocities greater than those expected after the conversion of the excitation energy and the complete redistribution of energy. In Figure 3 ($n = 4$–8), broad distributions at higher velocities are therefore evident that are clearly separated from the MB distribution. Fragmenting an individual water molecule requires high excitation energies (> 5.15 eV),[23] which could possibly be achieved in this high-energy experiment but would give rise to a different shape of the velocity distribution (see the Supporting Information).[19] The elusive nature of such dissociation events indicates that the excitation energy is at least partially converted, thus favoring redistribution.

Alternatively, a dissociative electronic excited state, which requires approximately 10 eV[24] (see also the Supporting Information),[19] would shift the velocity distributions towards higher values as the mass of the residue increases. Although such high excitation energies are also available in our experiment, they can also not account for the broad distributions. However, repeating the SMD simulations but localizing the excess energy on a single random molecule instead of the entire cluster indeed produces a much broader velocity distribution, with a high velocity tail that can be attributed to the excitation of the outer molecules (Figure 5). Excitation of the central hydronium ion, in contrast, only contributes to the MB part of the distribution. Repeating those simulations with the OSS2 model leads to essentially identical distributions, confirming the robustness of the present computational model.[19] The differences between uniform and local excitations highlight the incomplete energy redistribution in the high-velocity evaporation events and emphasize the role of chemistry on such non-ergodic events.

Therefore, the events observed here in the high-velocity range are a signature of evaporation occurring before energy redistribution can be fully achieved.[25] These non-ergodic events are in proportion of approximately 30% in the case of the tetramer. Nevertheless, complete energy redistribution, similar to that observed in macroscopic droplets, is dominant even for large excitation energies, thereby demonstrating the high thermalizing ability of water even at the nanoscopic scale. The small number of molecules involved in the present work paves the way towards systematic comparisons of classical, semi-classical, and even full quantum descriptions of the role of hydrogen bonding in energy transfer in such fields as atmospheric science,[26–27] astrochemistry,[28] and biology[29] in which radiation and its consequences may be responsible for both statistical and non-ergodic events.

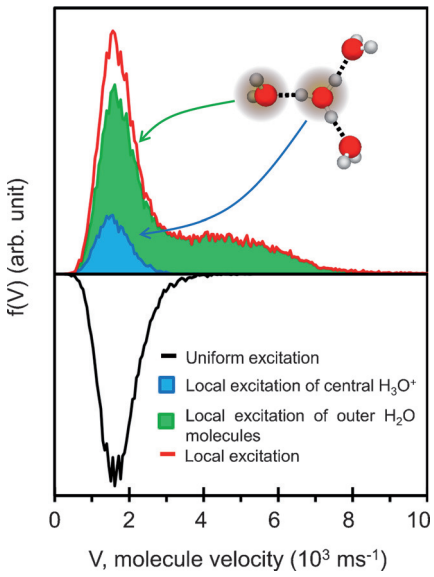

Figure 5. Velocity distributions for the tetramer obtained from localized excitations in the SMD model. Velocity distributions obtained for the unimolecular dissociation of H_2O from $H^+(H_2O)_4$, as simulated using the SMD model and assuming that the excitation is either distributed among all modes (black curve) or localized on a single random molecule (red curve). In the latter curve the contributions from the outer H_2O molecules and the central H_3O^+ are shown separately as green and blue histograms, respectively.

Acknowledgements

This work was supported by the Agence Nationale de la Recherche Française through grant numbers ANR-06-BLAN-0319 and ANR-10-BLAN-0411.

Keywords: energy transfer · mass spectrometry · molecular dynamics · velocity map imaging · water

How to cite: *Angew. Chem. Int. Ed.* **2015**, *54*, 14685–14689
Angew. Chem. **2015**, *127*, 14898–14902

[1] a) P. Ball, *Nature* **2008**, *452*, 291–292; b) R. Ludwig, *Angew. Chem. Int. Ed.* **2001**, *40*, 1808–1827; *Angew. Chem.* **2001**, *113*, 1856–1876; c) M. Olschewski, S. Knop, J. Lindner, P. Vöhringer, *Angew. Chem. Int. Ed.* **2013**, *52*, 9634–9654; *Angew. Chem.* **2013**, *125*, 9814–9836.
[2] M. L. Cowan, B. D. Bruner, N. Huse, J. R. Dwyer, B. Chugh, E. T. J. Nibbering, T. Elsaesser, R. J. D. Miller, *Nature* **2005**, *434*, 199–202.
[3] Z. Zhang, L. Piatkowski, H. J. Bakkerand, M. Bonn, *Nat. Chem.* **2011**, *3*, 888–893.
[4] G. Bruny, S. Eden, S. Feil, R. Fillol, K. El Farkh, M. M. Harb, C. Teyssier, S. Ouaskit, H. Abdoul-Carime, B. Farizon, M. Farizon, T. D. Märk, *Rev. Sci. Instrum.* **2012**, *83*, 013305.
[5] a) H. S. Lee, M. Kim, *J. Phys. Chem.* **1996**, *100*, 1459–1465; b) R. G. Cooks, *J. Mass Spectrom.* **1995**, *30*, 1215–1221; c) U. Saalmann, R. Schmidt, *Phys. Rev. Lett.* **1998**, *80*, 3213–3216.
[6] F. Remacle, R. D. Levine, *Proc. Natl. Acad. Sci. USA* **2006**, *103*, 6793–6798.
[7] B. Liu, S. B. Nielsen, P. Hvelplund, H. Zettergren, H. Cederquist, B. Manil, B. A. Huber, *Phys. Rev. Lett.* **2006**, *97*, 133401.
[8] M. H. Stockett, H. Zettergren, L. Adoui, J. D. Alexander, U. Bērziņs, T. Chen, M. Gatchell, N. Haag, B. A. Huber, P. Hvelplund, A. Johansson, H. A. B. Johansson, K. Kulyk, S. Rosén, P. Rousseau, K. Støchkel, H. T. Schmidt, H. Cederquist, *Phys. Rev. A* **2014**, *89*, 032701.
[9] L. C. Ch'ng, A. K. Samanta, G. Czakó, J. M. Bowman, H. Reisler, *J. Am. Chem. Soc.* **2012**, *134*, 15430–15435.
[10] S. Hayakawa, A. Kitaguchi, S. Kameoka, M. Toyoda, T. Ichihara, *J. Chem. Phys.* **2006**, *124*, 224320.

[11] G. E. Douberly, R. S. Walters, J. Cui, K. D. Jordan, M. A. Duncan, *J. Phys. Chem. A* **2010**, *114*, 4570 – 4579.
[12] V. V. Rybkin, A. O. Simakov, V. Bakken, S. Reine, T. Kjærgaard, T. Helgaker, E. Uggerud, *J. Comput. Chem.* **2013**, *34*, 533 – 544.
[13] E. Bruzzie, R. Parajuli, A. J. Stace, *Int. J. Mass Spectrom.* **2013**, *333*, 1 – 7.
[14] F. Berthias, V. Buridon, H. Abdoul-Carime, B. Farizon, M. Farizon, P. M. Dinh, P.-G. Reinhard, E. Suraud, T. D. Märk, *Phys. Rev. A* **2014**, *89*, 062705.
[15] M. Farizon, B. Farizon, H. Abdoul-Carime, G. Bruny, S. Eden, S. Feil, C. Montano, PCT/FR2010/052733, **2009**; WO 2011/080455, **2011**.
[16] C. Teyssier, R. Fillol, H. Abdoul-Carime, B. Farizon, M. Farizon, T. D. Märk, *Rev. Sci. Instrum.* **2014**, *85*, 015118.
[17] G. Brancato, M. E. Tuckerman, *J. Chem. Phys.* **2005**, *122*, 224507.
[18] M. Marciante, F. Calvo, *Mol. Simul.* **2014**, *40*, 176 – 184.
[19] See the Supporting Information: Method summary, evaporation of water molecules from $H^+(H_2O)_4$: a typical SMD event, a comparison of calculated distributions performed using SMD and OSS2 potential for molecules evaporated from the $H^+(H_2O)_4$ droplet, the potential-energy curves of the ground state, and the lowest electronically exited state of $H^+(H_2O)_2$, a possible contribution of intramolecular water dissociation as $H_2O \rightarrow H^{\cdot} + {}^{\cdot}OH$, a comparison of calculated distributions performed using SMD and OSS2 potential for molecules evaporated from the $H^+(H_2O)_4$ droplet in case of local excitation of a random individual molecule.
[20] L. Ojamae, I. Shavitt, S. J. Singer, *J. Chem. Phys.* **1998**, *109*, 5547 – 5564.
[21] A. K. Samanta, L. C. Ch'ng, H. Reisler, *Chem. Phys. Lett.* **2013**, *575*, 1 – 11 (see Figure 10 therein).
[22] P. Varilly, D. Chandler, *J. Phys. Chem. B* **2013**, *117*, 1419 – 1428.
[23] Y. R. Luo, *Comprehensive Handbook of Chemical Bond Energies*, CRC, Boca Raton, **2007**.
[24] S. Klein, E. Kochanski, A. Strich, A. J. Sadlej, *J. Phys. Chem. A* **1997**, *101*, 4799 – 4806.
[25] E. W. G. Diau, J. L. Herek, Z. H. Kim, A. H. Zewail, *Science* **1998**, *279*, 847 – 851.
[26] T. Berndt, J. Voigtländer, F. Stratmann, H. Junninen, R. L. Mauldin III, M. Sipilä, M. Kulmalab, H. Herrmanna, *Phys. Chem. Chem. Phys.* **2014**, *16*, 19130 – 19136.
[27] R. J. Buszek, J. S. Francisco, M. J. Anglada, *Int. Rev. Phys. Chem.* **2011**, *30*, 335 – 369.
[28] M. S. Westley, R. A. Baragiola, R. E. Johnson, G. A. Baratta, *Nature* **1995**, *373*, 405 – 407.
[29] T. W. Martin, Z. S. Derewenda, *Nat. Struct. Biol.* **1999**, *6*, 403 – 406.

Received: June 26, 2015
Revised: September 7, 2015
Published online: October 16, 2015

